Chapter 06. Results and Discussion

6.1 Preamble

The CFF reinforced PLA composite samples were prepared using two methods first a filament is prepared using a specially designed extruder and second using the sandwich method. The properties of the PLA granules used in manufacturing the samples are as shown in **Error! R eference source not found.** which was received from PLA supplier - CHEM TECH PRO, Vadodara.

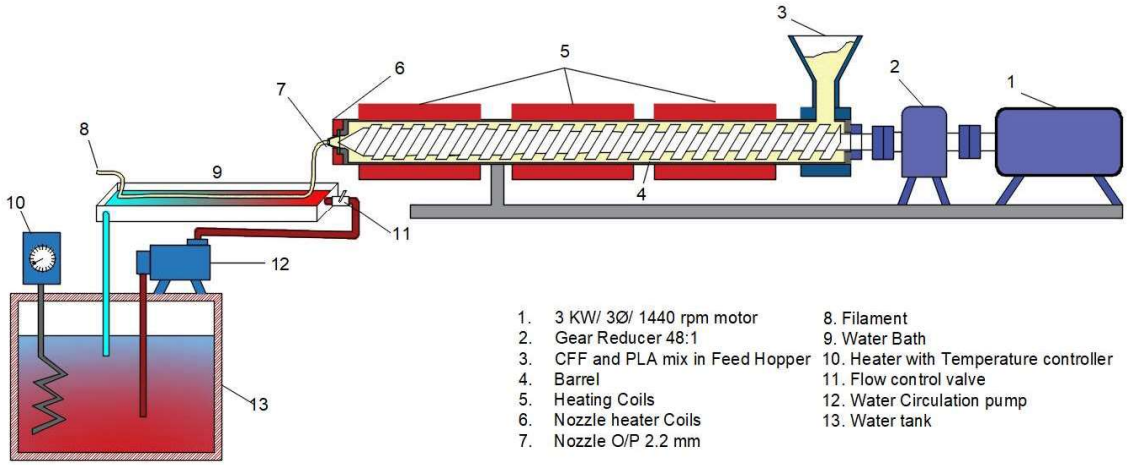

Figure 6-1 Schematic of the short fiber reinforced filament extruder.

The working parameters of the specially designed extruder are shown in Figure 6-1

Table 6-1 Controlled parameters for the specially designed filament extruder.

Parameter	Value
3 Ø Electric Motor driving frequency	35 Hz
Rotary speed of the extruder screw	22 rpm
The temperature of Heater 1	150°C
The temperature of Heater 2	134°C
The temperature of Heater 3	134°C
The temperature of the Nozzle Heater	140°C
The temperature of the water bath	75°C
Hot water flow rate	20 L/min
Nozzle diameter	2 mm

The length and diameter of the CFFs were measured as per ASTM D5103-07. The fiber length was obtained to have a value varying from 1.9 mm to 5.2 mm. This confirms that the fibers are

to be categorized as short length fibers. The average diameter of the barbs varied from 23 µm to 44 µm.

6.2 Test results of filament samples prepared using the filament extruder

Various tests were carried out to characterize the CFF/PLA samples. Subsequent sections present the results.

6.2.1 Tensile strength

The results of the tensile strength of the CFF/PLA filament samples are shown in Table 6-2 and presented graphically in Figure 6-2.

Table 6-2 Tensile characteristics of CFF/PLA filament samples.

Sample No	Ultimate Stress	Yield Stress	Break Stress
T 21	49.7	34.37	49.2
T 22	42.6	42.65	42.6
T 23	49.5	33.67	49.2
T 24	34.7	34.63	34.7
T 31	44.7	44.68	44.5
T 35	44.2	44.18	43.4

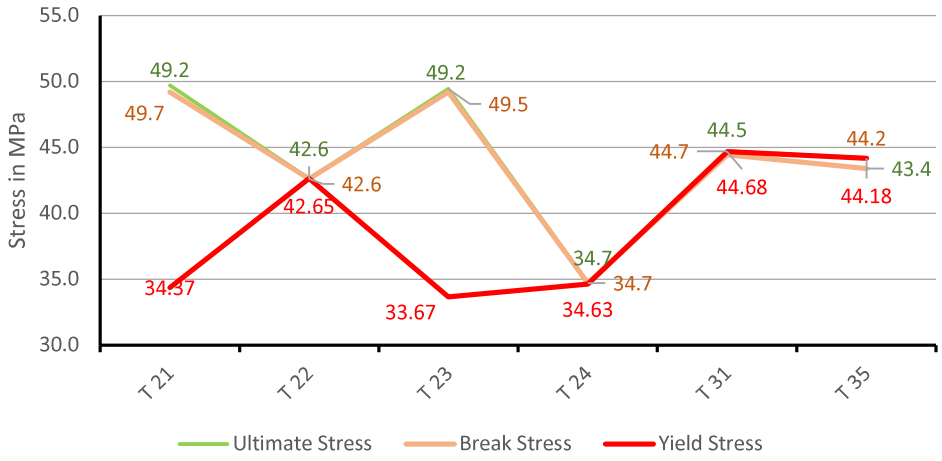

Figure 6-2 Tensile characteristics of CFF/PLA filament samples.

From the results, it is observed that in samples where maximum ultimate tensile and the break stress are observed that the yield strength is minimum. From the photographs of the point of failure as shown in Figure 6-4 reduction in diameter is observed. Comparatively, the presence of chicken in the region of failure is more. The presence of CFF, PLA and interactions at

interfaces are responsible for higher tensile strength. Table 6-3 presents a summary of the results from the tensile test reports. From the results, it is observed that the break stress is almost equal to the ultimate stress, which is indicative that the filament breaks as soon as it reaches ultimate stress. Also, there is no elongation.

Table 6-3 Summary of the tensile characteristics of CFF/PLA filament.

Values in MPa	Ultimate Stress	Yield Stress	Break Stress
Average	44.23	39.03	43.93
Minimum	34.72	33.67	34.72
Maximum	49.71	44.68	49.19

The tensile properties of 3D printed PLA were - Ultimate Stress: 32.94 MPa, Yield Stress: 35.90 MPa (Subramaniam et al., 2019). Compared to the 3D printed PLA the CFF/PLA composite filament samples show an increase of 34% in ultimate stress. Further investigations were done to justify the increase in tensile strength.

6.2.2 Visual Observation by stereoscopic microscope

The tensile tested samples were observed under a stereoscopic microscope NIKON SMZ1000 at 80x magnification to observe the conditions at the breakup points. Figure 6-3 shows the tensile tested samples under the stereoscopic microscope Nikon SMZ1000 at 80X magnification.

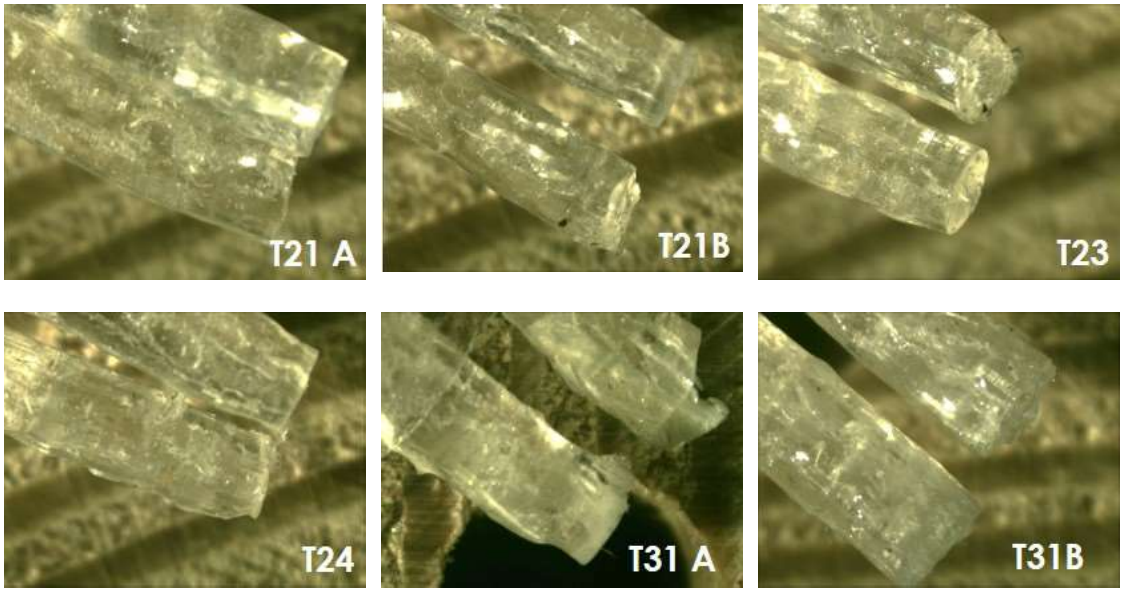

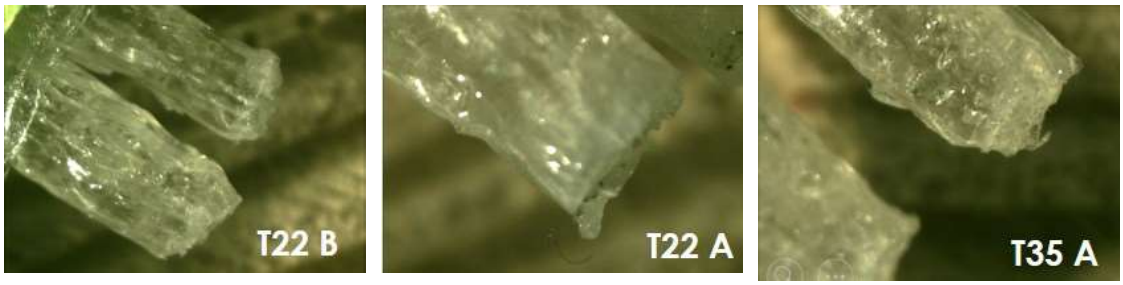

Figure 6-3 Observations of the tensile tested samples under the stereoscopic microscope. Nikon SMZ1000 at 80X magnification

Broken CFF and PLA fragments at the region of tensile failure as shown in Figure 6-4 are indicative of good interfacial bonding at the interfaces. Furthermore, from the image shown in Figure 6-5, a milky cloud-like formation is visible at the interfaces of CFF and PLA. The visual milky cloud-like substance indicates chemical interactions between CFF and PLA at the interfaces and the presence of polymorphs at the interfaces.

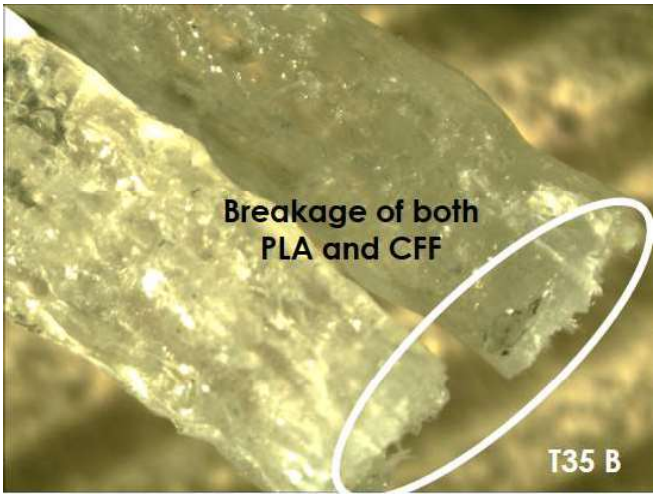

Figure 6-4 Breaking of CFF and PLA both at the breakup point of the filament sample at 100X magnification.

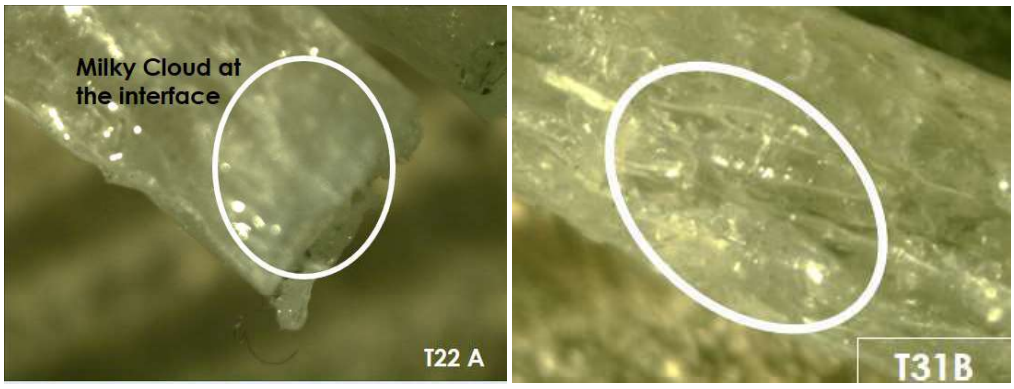

Figure 6-5 Milky cloud observed at the CFF/PLA interfaces at 100X magnification.

Although it is difficult to establish the presence of a polymorph by visual inspections, further investigations are necessary. DSC and TGA thermograms are methods to observe and establish the presence of third compound/ chemical interactions at the interfaces.

The diameter of the manufactured CFF/PLA composite filament was also measured under the stereoscopic microscope. The average diameter of the filament was observed between 2.18 mm to 2.21 mm. Although the nozzle diameter was 2 mm, the composite filament diameter was obtained at an average of 2.2 mm. This is an increase in the diameter. When compressed molten plastic is forced out through a nozzle, initially the viscous mixture of the material is compressed because of the pressure created by the screw inside the barrel. Later after coming out of the nozzle, the material expands freely, resulting in the filament with a higher diameter. The expansion can be controlled by controlling the RPM of the screw and the temperature profile inside the barrel. The higher the temperature, the lesser would be the diameter of the filament. The temperature ranges before its melting temperature (~ 6-7 °C), and the behavior of the PLA is highly viscous. As soon as the temperature reaches melting temperature, the material becomes fluid and it cannot be used for extrusion. To obtain the filament of required size further process can be carried out at lower temperatures. This can be the basis for future work.

6.2.3 Differential Scanning Calorimetry (DSC)

The thermal behaviour of the CFF/PLA filament was studied from the DSC curves. Figure 6-6 depicts the DSC thermogram curve of CFF/PLA filament samples.

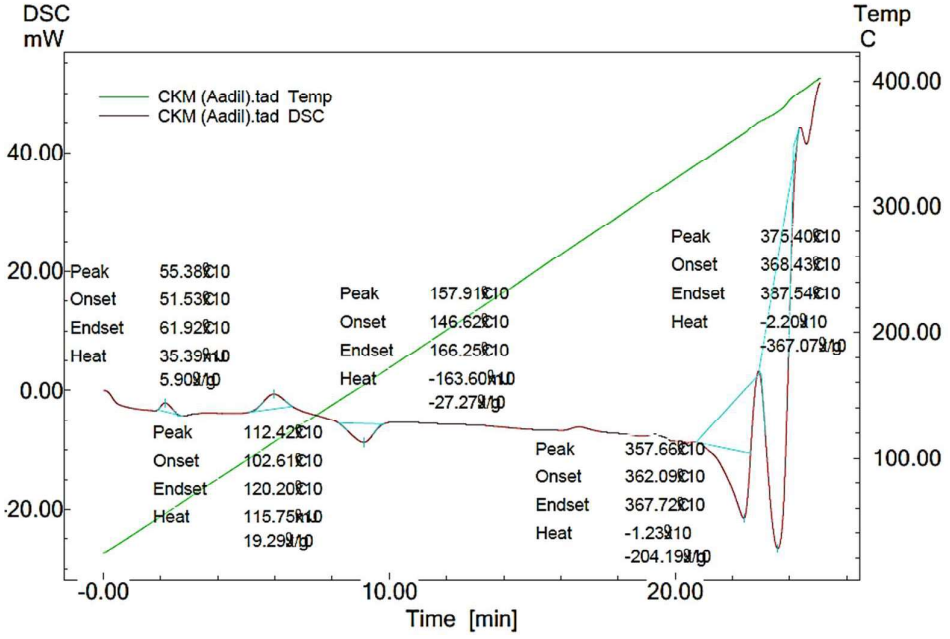

Figure 6-6 DSC curves of CFF/PLA filament sample.

Table 6-4 presents a summary of the peaks found in the DSC curves of CFF/ PLA composite filament. It is observed that the glass transition temperature (Tg) increased as compared to base materials (i.e. CFF and PLA), which may be attributed to the increase in tensile strength and the presence of polymorphs formed at the interfaces. It is also indicative of chemical reactions and bonding at the interfaces of CFF and PLA in the composite filament.

Table 6-4 Summary of the thermal peaks found in DSC curves of CFF/PLA filament as shown in Figure 6-6.

Peak No	Peak	Onset	Endset	Heat
1	55.38 °C	51.53 °C	61.92 °C	35.39mJ
2	112.42 °C	102.61 °C	120.20 °C	115.75 mJ
3	157.91 °C	146.62 °C	166.25 °C	-163.60mJ
4	357.66 °C	362.09 °C	367.72 °C	-1.23 J
5	375.40 °C	368.43 °C	387.54 °C	-2.20 J

Peak 1 corresponds to Tg of PLA which is around 50-55°C. The second peak corresponds to the temperature range where the water in bonded and unbonded form is removed. Corresponding to the DSC curves of PLA and CFF in Figure 6-7, it can be inferred that the breakage of the crystalline structure of CFF corresponds to the third peak. The fourth peak does not correspond to any of the temperature peaks corresponding to the PLA or CFF as shown in Figure 6-7. In the DSC of CFF/PLA filaments, between the temperatures 357 °C and 387.54 °C, two peaks are observed. In these peaks, there is a change from an endothermic to an exothermic process and vice versa, which is an indication of the breaking of two different crystalline structures. The existence of the fourth peak and the fifth peak indicates the breakage of another crystalline structure which is neither corresponding to CFF nor Poly-Lactic Acid. This behavior is elucidated to the free volume concept: where free molecules in one material occupy gaps in another material chain structure, increasing rigidity. The specific volume decreases resulting in a higher thermal energy required to break the crystalline structure (Wu et al., 2014).

The increased Tg can also be accounted to the interaction between the amide groups and the rich oxygen functionalities present in PLA. It improved the interfacial interaction between the oxygen reaching the Carbon chain of PLA with the nitrogen rich Amides and amines in the presence of sulphones and sulphonates present in CFF (Tesfaye, Sithole, Ramjugernath, and Chunilall, 2017). The increase in tensile strength can be attributed to the presence of these interactions. This further leads to conform the increase in the tensile strength and presence of

another polymorph in the composite filament compared to base materials. A similar interpretation has been presented by Zhang et al (Zhang et al., 2019).

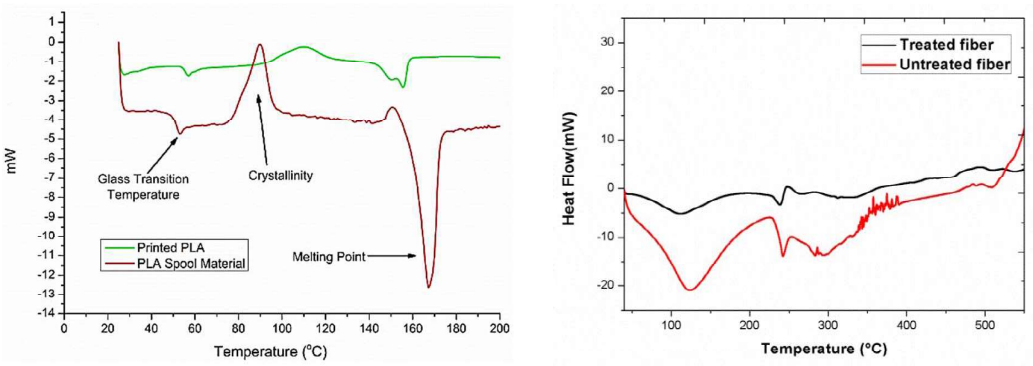

(a) (b)

Figure 6-7 DSC curves of (a) PLA and (b) CFF.

The glass transition temperature of PLA is 57 °C and of CFF is 315 °C, while in the prepared sample it is observed between 357 °C and 387 °C. Another indication of the possibility of crosslinking at the interfaces and formation of enhanced compound material.

6.2.4 Thermogravimetric Analysis (TGA)

TGA and Derivative TGA (DTA) are used to obtain the composition of samples and predict the thermal stability at different temperatures. Thermogravimetric analysis of CFF/PLA filament samples was carried out according to ASTM E1131. The TGA thermograms of the composite filaments are displayed in Figure 6-8.

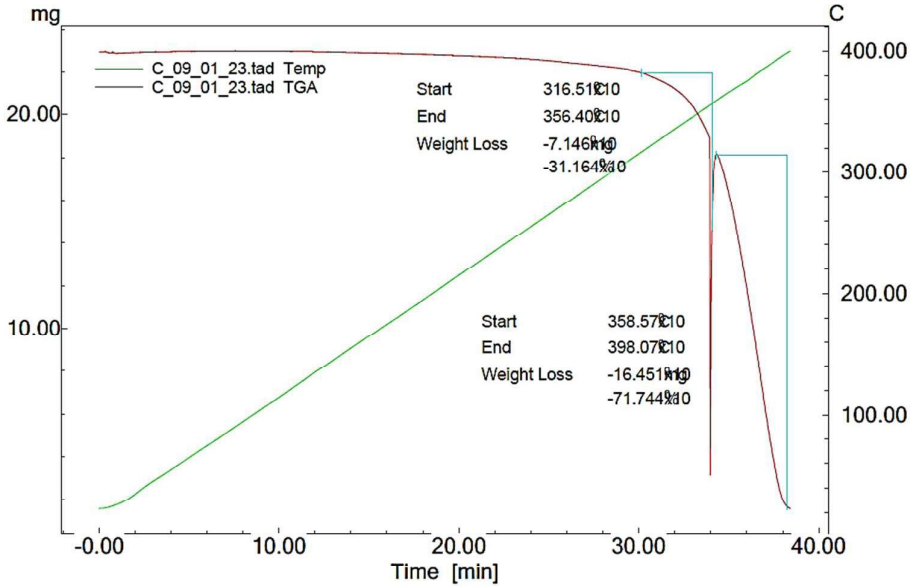

Figure 6-8 TGA of CFF/PLA filament.

The TGA curves in Figure 6-8 indicate that till the temperature of 316.5 °C there was a weight loss of only 4.5%. Between 316.5 °C to 356.4 °C further 30% of weight loss was observed. The curve at this point is indicative of thermal decomposition with the formation of gaseous products such as CO_2 and CO. From 356.4 °C to 359.03 °C there was a weight gain of about 9%. This might be accredited to the endothermic behavior and absorbance of oxygen before the breaking of another crystalline structure. The curve indicates explosive decomposition with a recoil. This seconds the conclusion of the breakage of the secondary crystalline structure near 359 °C. Between 359.03 °C to 398 °C, 75% of the complete degradation of the material was observed. This loss occurs after the breakage of the crystalline structure. 1% i.e. about 1.56 grams of unburnt residue remained at the end of the test.

The crystalline structure is more stable than the parent materials. The same is inferred from the difference in slope of denaturing and degradation as compared to that observed in CFF and PLA individually. The TGA curves of Chicken feather and PLA is shown in Figure 6-9.

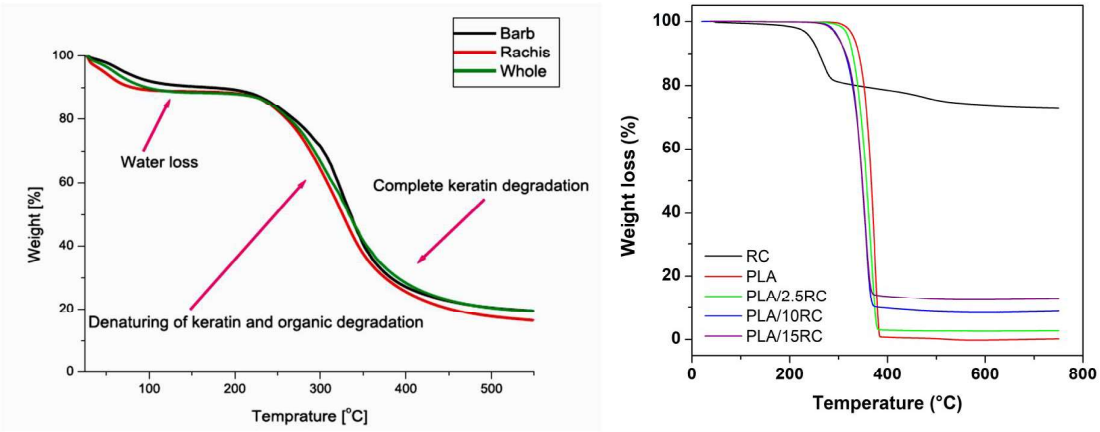

(a) (b)

Figure 6-9 TGA thermograms of (a) CFF and (b) PLA.

From the TGA we can say that the thermal resistivity and stability have increased. The endothermic behaviour observed near 355°C is further confirmed by carrying out derivative TGA (DTGA) of the TGA results. The sudden drop in TGA and DTGA is also indicative of sample melting with decomposition. The DTGA shown in Figure 6-10 was plotted using OriginPro software. This might be due to the rigid polymorph formed at the interfaces of CFF and PLA in the composite filament.

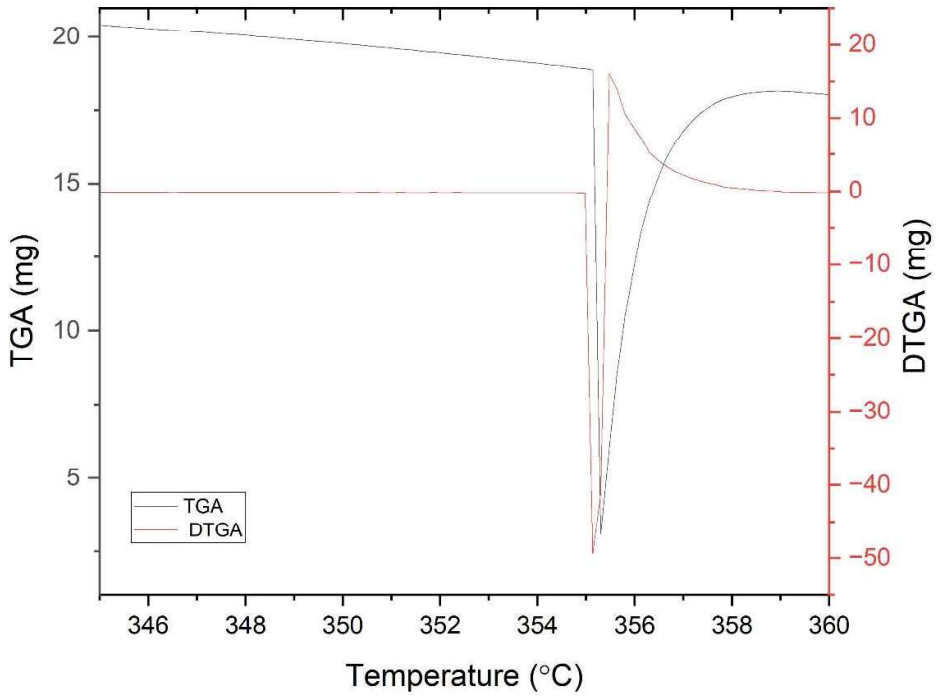

Figure 6-10 TGA and DTGA of CFF/PLA composite filament in the temperature region 345°C to 360°C.

From the thermal behaviour observed from DSC and TGA curves, it is conclusive that there is a presence of chemical bonding at the interfaces of CFF and PLA and the formation of polymorphs. The determination of the chemical compounds formed is inferred from FT-IR measurements.

6.2.4 Fourier transform infrared spectroscopy (FT-IR)

The FT-IR measurements were carried out as per ASTM E168. Figure 6-11 shows the FT-IR measurements of the CFF/PLA filament sample. The FT-IR of composite filament in Figure 6-11 shows strong intermolecular hydroxyl (O-H) bonds, alkene (C=C), alkyne, alkane, aldehyde, isothiocyanate, allene, anhydrides – conjugated anhydrides, Sulfonates-Sulfone (S=O), ester bonds along with amide/amine (C-N-H) bonds. the FT-IR measurements of CFF reported in earlier research (Tesfaye, Sithole, Ramjugernath, and Chunilall, 2017) showed peaks of only Amide (Figure 6-12).

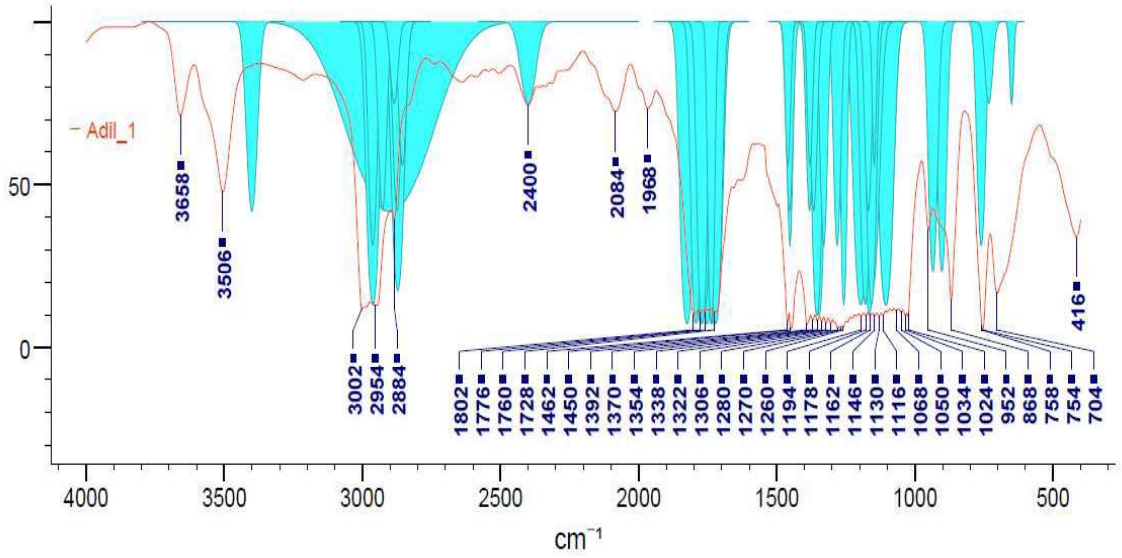

Figure 6-11 FT-IR measurements of CFF/PLA filament samples.

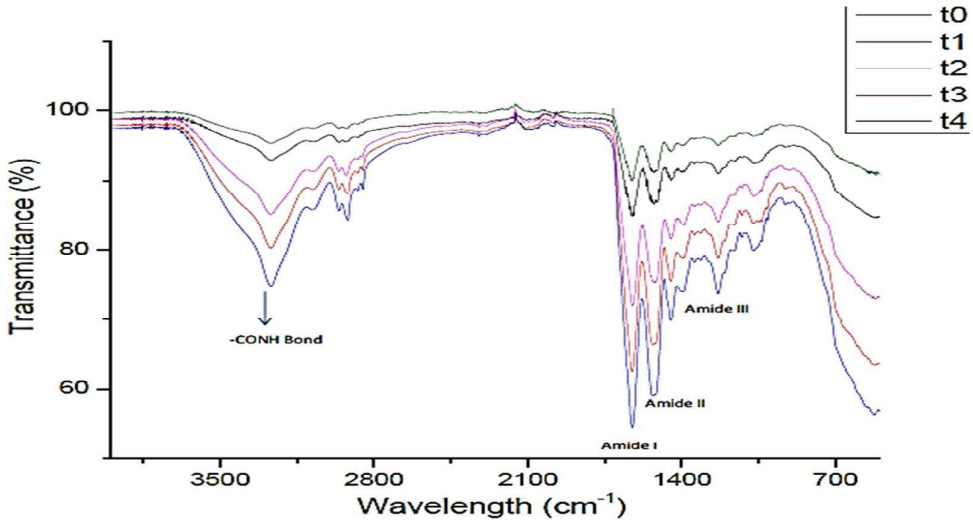

Figure 6-12 FT-IR measurements of CFF.

The Sulfonates-Sulfone (S=O), ester bonds along with amide/amine (C-N-H) bonds indicate chemical compound exchanges at the interfaces. The presence of isothiocyanate and sulfonates also indicate a strong possibility of crosslinking between CFF and PLA molecules. (Webb et al., 2013). The crosslinking and chemical interactions at the interfaces have resulted in enhanced physical properties. The interface exchanges are not just by wetting and absorption as observed with other composite compounds.

6.2.5 Solubility in Alkaline Medium

Biomaterials are soluble in acidic medium. (Deshayes and Kasko, 2013). CFF and PLA both being biomaterials are also soluble in acidic medium. It is not necessary for biomaterials to be soluble in an alkaline medium. Thus, the CFF/PLA composite filament was tested for solubility in an alkaline medium. 5% by weight NaOH dilute solution was selected for testing (Fitriyanto et al., 2022). The weight of the filament used was 1 gm. Chicken feather was diluted in the solution after heating it at a boiling temperature of solution i.e. 96 °C for about 4 hours. The composite filament was also immersed in the solution and boiled till the entire water in the solution was evaporated but no changes were observed. Further, the same sample was immersed by adding 5% by weight NaOH solution and kept at room temperature for 48 hours still, no changes were observed. After 48 hours again the solution was reheated at boiling temperature. During this process, the material at the interfaces was partially dissolved while the chicken feather was dissolved.

Dissolved CFF solution and semi-dissolved composite solution were observed under the BRL-295 spectrometer. In both cases, only one peak was observed i.e. at 242 nm. This confirmed that in the composite sample, only the chicken feather was dissolved. Since the filaments used were cut and all the compounds i.e. CFF, PLA, and compounds formed at interfaces were subjected to an alkaline medium and only CFF is dissolved it shows the stability which can be achieved and widens the application of the filament to manufacture 3D printed parts subjected to alkaline medium.

6.2.6 Electrical Resistance

The filaments were tested for their electrical resistance. First direct resistance was measured using a multimeter. The filament piece was connected across AC and DC and the voltage was varied from $0 - 230$V.

The samples were connected to the two terminals and supplied with AC and DC voltage. The measurement was observed using an M65 multimeter (Motwane make). The resistance shown was greater than 60 MΩ. When subjected to potential difference from 0 V to 260 V both AC and DC, the filament sample showed no changes. It confirms that the composite material retains the insulating properties of both the base materials i.e. Chicken feather(Tesfaye, Sithole, Ramjugernath, Chunilall, et al., 2017) and Poly-lactic Acid (PLA) (Shinyama, 2018).